APECSS

(Acoustic Pulse Emitted by Cavitation in Spherical Symmetry)

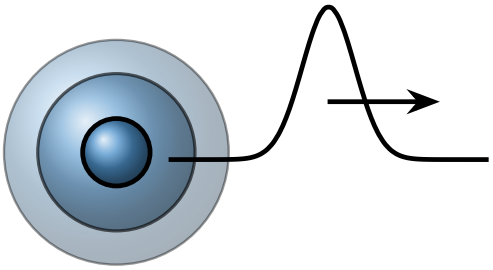

Fabian Denner
Sören Schenke

17 October 2022

Contents

Chapter 1

About APECSS

APECSS is a software tool to compute pressure-driven bubble dynamics and the resulting acoustic emissions. It is written exclusively in C and has been developed with simplicity, versatility and performance in mind. The acronym APECSS stands for "Acoustic Pulse Emitted by Cavitation in Spherical Symmetry".

The development of APECSS has directly benefitted from research funding provided by the Deutsche Forschungsgemeinschaft (DFG, German Research Foundation), grant number 441063377.

1.1 Overview

1.2 Project structure

Chapter 2

Using APECSS

2.1 Installation

2.2 Run options

2.3 Programming in APECSS

All routines are placed in source files that relate to parts of the code, distinguished by physical phenomena (e.g. `nonspherical.c`), fluid type (e.g. `liquid.c`) or computational operations (e.g. `results.c`). All decalarations and definitions are located in the header file `apecss.h`.

To ensure a consistent formatting, please use a clang formatter that formats the file automatically upon saving. The file defining the formatting of the APECSS source code (`.clang-format`) is part of the respository.

2.3.1 Macros

Macros are used as shortcuts to define frequently-used constants (e.g. `APECSS_PI`), for frequently-used computational operations (e.g. `APECSS_MAX`) and for computational operations that depend on the chosen machine precision (e.g. `APECSS_SIN`). Furthermore, options related to different numerical models are represented by logically named flags.

2.3.1.1 Macros related to machine precision

APECSS can be used with different floating point precisions: double precision (default) and long double precision (`APECSS_PRECISION_LONGDOUBLE`).

Based on the chosen precision, `APECCS_FLOAT` is defined as the standard floating point type. In addition, the following precision-dependent computational operations are defined based on the chosen floating point precision:

- `APECSS_ABS(a)`: Absolute value of a.
- `APECSS_CEIL(a)`: a rounded to the nearest integer larger than a.
- `APECSS_COS(a)`: Cosine of a.
- `APECCS_EPS`: Reference value that is close to machine zero.
- `APECSS_EXP(a)`: e to the power a.
- `APECSS_LOG(a)`: Natural logarithm of a.

- `APECSS_POW(a,b)`: Power b of a.
- `APECSS_SIN(a)`: Sine of a.
- `APECSS_SMALL`: A very small number significantly smaller than machine precisionn
- `APECSS_SQRT(a)`: Square root of a.
- `APECSS_STRINGTOFLOAT(a)`: Conversion of a string to float a.

To ensure compatibility for different floating point precisions, it is paramount to use the standard floating point type `APECCS_FLOAT` and the operator definitions given above consistently throughout APECSS.

2.3.1.2 Computational operations and predefined constants

Macros that provide a shortcut to frequently-used computational operations are:

- `APECSS_POW2(a)`: Returns a^2
- `APECSS_POW3(a)`: Returns a^3
- `APECSS_POW4(a)`: Returns a^4
- `APECCS_MAX(a,b)`: Returns the maximum of a and b.
- `APECSS_MAX3(a,b,c)`: Returns the maximum of a, b and c.
- `APECSS_MIN(a,b)`: Returns the minimum of a and b.
- `APECSS_MIN3(a,b,c)`: Returns the minimum of a, b and c.

Macros that provide a shortcut to frequently-used constants are:

- `APECSS_PI`: Returns π
- `APECSS_E`: Returns e
- `APECSS_ONETHIRD`: Returns $1/3$
- `APECSS_ONESIXTH`: Returns $1/6$
- `APECCS_AVOGADRO`: Returns the Avogadro constant.
- `APECSS_LN_OF_2`: Returns the natural logarithm of 2.
- `APECSS_LN_OF_10`: Returns the natural logarithm of 10.

2.3.1.3 Flags for model options

All model options are represented by human-readable flags. Many of these flags are defined in such a way (with integer values being a multiple of 2), that a bit-wise comparison can be performed. Bit-wise comparison are used for options that are checked frequently and for options that can have several building blocks.

Options of the Runge-Kutta scheme used to discretize the ODEs:

- `APECSS_RK54_7M`: RK5(4)7M (minimum truncation) coefficients of Dormand and Prince [3]
- `APECSS_RK54_7S`: RK5(4)7S (stability optimized) coefficients of Dormand and Prince [3]

Rayleigh-Plesset schemes:

- `APECSS_BUBBLEMODEL_RP`: Standard Rayleigh-Plesset model, (3.1)
- `APECSS_BUBBLEMODEL_RP_ACOUSTICRADIATION`: Rayleigh-Plesset model incl. acoustic radiation term, (3.2)
- `APECSS_BUBBLEMODEL_KELLERMIKSIS`: Keller-Miksis model, (3.3)
- `APECSS_BUBBLEMODEL_GILMORE`: Gilmore model, (3.4)

Equation-of-state of the gas:

- `APECSS_GAS_IG`: Ideal gas

- `APECSS_GAS_HC`: Ideal gas with van-der-Waals hardcore
- `APECSS_GAS_NASG`: Noble-Abel-stiffened-gas

Viscoelasticity of the liquid:

- `APECSS_LIQUID_NEWTONIAN`: Newtonian liquid
- `APECSS_LIQUID_KELVINVOIGT`: Kelvin-Voigt solid
- `APECSS_LIQUID_ZENER`: Zener solid (standard linear solid model)
- `APECSS_LIQUID_OLDROYDB`: Oldroyd-B liquid

Lipid monolayer coating of the gas-liquid interface:

- `APECSS_LIPIDCOATING_NONE`: No lipid monolayer coating
- `APECSS_LIPIDCOATING_MARMOTTANT`: Lipid monolayer coating described by the model of Marmottant *et al.* [9]
- `APECSS_LIPIDCOATING_GOMPERTZFUNCTION`: Redefine the Marmottant model with a Gompertz function [5].

Acoustic excitation applied to the bubble:

- `APECSS_EXCITATION_NONE`: No external excitation.
- `APECSS_EXCITATION_SIN`: Sinusoidal excitation.

Model to compute the acoustic emissions of the bubble:

- `APECSS_EMISSION_NONE`: Emissions are not modelled.
- `APECSS_EMISSION_INCOMPRESSIBLE`: Emissions are assumed to occur in an incompressible fluid.
- `APECSS_EMISSION_FINITE_TIME_INCOMPRESSIBLE`: Emissions are assumed to occur in an incompressible fluid, but the finite propagation speed given by the speed of sound is taken into account.
- `APECSS_EMISSION_QUASIACOUSTIC`: Emissions are modelled under the quasi-acoustic assumption of Gilmore [4].
- `APECSS_EMISSION_KIRKWOODBETHE`: Emissions are modelled based on the Kirkwood-Bethe hypothesis,

2.3.1.4 Others

Other predefined macros are used to define the verbosity of APECSS, the length of strings and arrays, as well as to help with debugging:

- `APECSS_DATA_ALLOC_INCREMENT`: The increment for dynamics re-allocation of arrays.
- `APECSS_STRINGLENGTH`: The standard length of a string.
- `APECSS_STRINGLENGTH_SPRINTF`: The standard length of a string to written out in the terminal.
- `APECSS_STRINGLENGTH_SPRINTF_LONG`: The standard length of a long string to written out in the terminal.
- `APECSS_WHERE`: Outputs in the terminal the file name and line number where the macro is called.
- `APECSS_WHERE_INT(a)`: Outputs in the terminal the file name and line number where the macro is called, plus the integer value a.
- `APECSS_WHERE_FLOAT(a)`: Outputs in the terminal the file name and line number where the macro is called, plus the floating point value a.

2.3.2 Structures

Chapter 3

Bubble dynamics

The dynamic behaviour of the bubble is modelled with a Rayleigh-Plesset-type model, assuming spherical symmetry. This requires to choose a suitable RP-model (Section 3.1) and define appropriate conditions for the gas (Section 3.2), the liquid (Section 3.3), the interface (Section 3.4), as well as at infinity (Section 3.5). Optionally, nonspherical modes of the bubbel may be simulated (Section **??**) may be modelled.

3.1 Rayleigh-Plesset models

APECSS offers four Rayleigh-Plesset-type models to simulate pressure-driven bubble dynamics: the standard Rayleigh-Plesset model without and with acoustic radiation damping, the Keller-Miksis model and the Gilmore model.

Section	Command	Description
`BUBBLE`	`RPModel RP`	Standard Rayleigh-Plesset model, Eq. (3.1) (default: `RP`).
	`RPModel RPAR`	Rayleigh-Plesset model with acoustic radiation damping, Eq. (3.2) (default: `RP`).
	`RPModel KM`	Keller-Miksis model, Eq. (3.3) (default: `RP`).
	`RPModel Gilmore`	Gilmore model, Eq. (3.4) (default: `RP`).

The standard Rayleigh-Plesset (RP) model is given as [7]

$$R\ddot{R} + \frac{3}{2}\dot{R}^2 = \frac{p_\mathrm{L} - p_\infty}{\rho_\ell}, \tag{3.1}$$

where R is the bubble radius, p_L is the pressure of the liquid at the bubble wall, p_∞ is the pressure of the liquid at infinite distance from the bubble, p_G is the pressure of the gas inside the bubble and ρ_ℓ is the *constant* density of the liquid.

To incorporate acoustic radiation in the liquid and the associated damping, a modified Rayleigh-Plesset model is given as [1]

$$R\ddot{R} + \frac{3}{2}\dot{R}^2 = \frac{p_\mathrm{L} - p_\infty}{\rho_\ell} + \frac{R\,\dot{p}_\mathrm{G}}{\rho_\ell\, c_\ell}, \tag{3.2}$$

where the last term on the right-hand side accounts for acoustic radiation in the liquid. This modified RP model is frequently used to simulate medical ultrasound applications [15] as well as sonoluminescence [1]. It follows directly from the Keller-Miksis model, Eq. (3.3), which incorporates the compressibility of the liquid, by assuming the Mach number of the bubble wall is small, $M_\ell = \dot{R}/c_\ell \ll 1$.

Eq. (3.2) is, consequently, only valid for small Mach numbers $M_\ell = \dot{R}/c_\ell \ll 1$ [10, 12], although feasible results have frequently been obtained with Eq. (3.2) for Mach numbers $M_\ell \sim 1$ [1].

The Keller-Miksis model [6, 12], which incorporates the compressibility of the liquid to first order, is given as

$$\left(1-\frac{\dot{R}}{c_\ell}\right) R\ddot{R} + \frac{3}{2}\left(1-\frac{\dot{R}}{3\,c_\ell}\right)\dot{R}^2 = \left(1+\frac{\dot{R}}{c_\ell}\right)\frac{p_\mathrm{G}-p_\infty}{\rho_\ell} + \frac{p_\mathrm{L}-p_\mathrm{G}}{\rho_\ell} + \frac{R\,\dot{p}_\mathrm{G}}{\rho_\ell\,c_\ell}, \tag{3.3}$$

where c_ℓ is the speed of sound of the liquid. Both ρ_ℓ and c_ℓ are assumed to be constant.

Based on the Kirkwood-Bethe hypothesis, Gilmore [4] derived a second-order ordinary differential equation describing the radial dynamics of a bubble in a compressible liquid,

$$\left(1-\frac{\dot{R}}{c_\mathrm{L}}\right) R\ddot{R} + \frac{3}{2}\left(1-\frac{\dot{R}}{3c_\mathrm{L}}\right)\dot{R}^2 = \left(1+\frac{\dot{R}}{c_\mathrm{L}}\right) H + \left(1-\frac{\dot{R}}{c_\mathrm{L}}\right)\frac{R\dot{H}}{c_\mathrm{L}}, \tag{3.4}$$

where the subscript L denotes quantities of the liquid at the bubble wall ($r = R$), and with $H = h_\mathrm{L} - h_\infty$ and $\dot{H} = \dot{h}_\mathrm{L} - \dot{h}_\infty$. The enthalpy h and the speed of sound c are defined by an appropriate equation of state as a function of pressure, with $h_\mathrm{L} = h(p_\mathrm{L})$, $h_\infty = h(p_\infty)$ and $c_\mathrm{L} = c(p_\mathrm{L})$, detailed in **??**.

3.2 The gas

Section	Command	Description
`GAS`	`EOS IG`	Ideal gas model (default: `IG`).
	`EOS HC`	Ideal gas model with van-der-Waals hardcore (default: `IG`).
	`EOS NASG`	Noble-Abel-stiffened-gas model [8] (default: `IG`).
	`PolytropicExponent <float>`	Polytropic exponent Γ_g
	`ReferencePressure <float>`	Reference pressure $p_\mathrm{g,ref}$
	`ReferenceDensity <float>`	Reference density $\rho_\mathrm{g,ref}$
	`ReferenceTemperature <float>`	Reference temperature $T_\mathrm{g,ref}$
	`HardcoreRadius <float>`	Hardcore radius r_hc
	`CoVolume <float>`	Co-volume b_g
	`TaitPressureConst <float>`	Pressure constant B_g
	`MolecularWeight <float>`	Molecular weight $\mathcal{M}_\mathrm{g}$ of a gas molecule
	`MolecularDiameter <float>`	Kinematic diameter $\mathcal{D}_\mathrm{g}$ of a gas molecule

Using the ideal gas model, the pressure and its derivative are given as

$$p_\mathrm{G} = p_\mathrm{G,0}\left(\frac{\rho}{\rho_\mathrm{g,0}}\right)^{\Gamma_\mathrm{g}} \tag{3.5}$$

$$\dot{p}_\mathrm{G} = \frac{\dot{\rho}_\mathrm{G}\,\Gamma_\mathrm{g}\,p_\mathrm{G}}{\rho_\mathrm{G}}, \tag{3.6}$$

$$\tag{3.7}$$

including a van-der-Waals hardcore in the ideal gas model, the pressure and its derivative follow as

$$p_\mathrm{G} = p_{\mathrm{G},0} \left(\frac{\rho^3 - r_\mathrm{hc}^3}{\rho_{\mathrm{g},0}^3 - r_\mathrm{hc}^3} \right)^{\Gamma_\mathrm{g}} \tag{3.8}$$

$$\dot{p}_\mathrm{G} = -3 \frac{p_\mathrm{G}\, \Gamma_\mathrm{g}\, R^2\, \dot{R}}{R^3 - r_\mathrm{hc}^3}, \tag{3.9}$$

and using the Noble-Abel-stiffened-gas model, the pressure and its derivative are [2]

$$p_\mathrm{G} = (p_{\mathrm{G},0} + B_\mathrm{g}) \left[\frac{\rho_\mathrm{g}\,(1 - b_\mathrm{g}\,\rho_{\mathrm{g},0})}{\rho_{\mathrm{g},0}\,(1 - b_\mathrm{g}\,\rho_\mathrm{G})} \right]^{\Gamma_\mathrm{g}} - B_\mathrm{g} \tag{3.10}$$

$$\dot{p}_\mathrm{G} = \frac{\dot{\rho}_\mathrm{G}\, \Gamma_\mathrm{g}\, (p_\mathrm{G} + B_\mathrm{g})}{\rho_\mathrm{G}\,(1 - b_\mathrm{g}\,\rho_\mathrm{G})} \tag{3.11}$$

For all three equations of state, the the gas density and its derivative are given by

$$\rho_\mathrm{G} = \rho_{\mathrm{g},0} \left(\frac{R_0}{R} \right)^3 \tag{3.12}$$

$$\dot{\rho}_\mathrm{G} = -3\,\rho_\mathrm{G}\,\frac{\dot{R}}{R}. \tag{3.13}$$

3.3 The liquid

Section	Command	Description
`LIQUID`	`LiquidType Newtonian`	Newtonian fluid (default: `Newtonian`).
	`LiquidType KelvinVoigt`	Kelvin-Voigt solid (default: `Newtonian`).
	`LiquidType Zener`	Zener solid (default: `Newtonian`).
	`LiquidType OldroydB`	Oldroyd-B fluid (default: `Newtonian`).
	`PolytropicExponent <float>`	Polytropic exponent Γ_ℓ
	`ReferencePressure <float>`	Reference pressure $p_{\ell,\mathrm{ref}}$
	`ReferenceDensity <float>`	Reference density $\rho_{\ell,\mathrm{ref}}$
	`ReferenceSpeedofSound <float>`	Reference speed of sound $\rho_{\ell,\mathrm{ref}}$
	`HardcoreRadius <float>`	Hardcore radius r_hc
	`CoVolume <float>`	Co-volume b_g
	`TaitPressureConst <float>`	Pressure constant B_g
	`Viscosity <float>`	Viscosity μ_ℓ
	`PolymerViscosity <float>`	Polymer viscosity η_ℓ associated with viscoelasticity
	`ShearModulus <float>`	Shear modulus G_ℓ associated with viscoelasticity
	`RelaxationTime <float>`	Relaxation time λ_ℓ associated with viscoelasticity

The pressure at the bubble wall of a Newtonian liquid is given as

$$p_\mathrm{L} = p_\mathrm{G} - \frac{2\sigma}{R} - 4\,\mu_\ell \frac{\dot{R}}{R}, \tag{3.14}$$

where p_G is the gas pressure, see Section 3.2, σ is the surface tension coefficient of the interface, see Section 3.4, and μ_ℓ is the liquid viscosity.

For the Gilmore model (3.4), an equation-of-state (EoS) for the liquid has to be defined to determine the density ρ_L and the speed of sound c_L. Since the seminal work of Gilmore [4], the Tait EoS is traditionally used to describe the properties of the liquid in Eq. (3.4). The Tait EoS defines the

density ρ, enthalpy h and speed of sound c as

$$\rho = \rho_0 \left(\frac{p+B}{p_0+B} \right)^{\frac{1}{\Gamma}} \tag{3.15}$$

$$h = \frac{\Gamma}{\Gamma-1} \frac{p+B}{\rho} \tag{3.16}$$

$$c = \sqrt{\Gamma \frac{p+B}{\rho}}, \tag{3.17}$$

respectively, where B is a pressure constant, Γ is the polytropic exponent, p_0 is the reference pressure and ρ_0 is the reference density. For water, typical values for the pressure constant and the polytropic exponent are $B = 3.046 \times 10^8$ Pa and $\Gamma = 7.15$ [4]. However, the Tait EoS cannot provide physically-meaningful temperature values [13]. Using the Noble-Abel stiffened-gas (NASG) EoS [8] instead of the Tait EoS, the fluid properties are defined as [2]

$$\rho = \frac{K\,(p+B)^{\frac{1}{\Gamma}}}{1+b\,K\,(p+B)^{\frac{1}{\Gamma}}} \tag{3.18}$$

$$h = \frac{\Gamma}{\Gamma-1} \frac{p+B}{\rho} - \frac{\Gamma\, b}{\Gamma-1}\,(p+B) + b\,p, \tag{3.19}$$

$$c = \sqrt{\Gamma \frac{(p+B)}{\rho - b\rho^2}}, \tag{3.20}$$

with $K = \rho_0/[(p_0+B)^{1/\Gamma}\,(1-b\rho_0)]$ describing a constant reference state, and where b is the co-volume of the liquid molecules. The NASG EoS reduces to the Tait EoS for $b = 0$.

3.4 The interface

Section	Command	Description
INTERFACE	`GasEOS IG`	Ideal gas model (default: `IG`).
	`GasEOS HC`	Ideal gas model with van-der-Waals hardcore (default: `IG`).
	`GasEOS NASG`	Noble-Abel-stiffened-gas model (default: `IG`).
	`PolytropicExponent <float>`	Polytropic exponent Γ_g
	`ReferencePressure <float>`	Reference pressure $p_\mathrm{g,ref}$
	`ReferenceDensity <float>`	Reference density $\rho_\mathrm{g,ref}$
	`ReferenceTemperature <float>`	Reference temperature $T_\mathrm{g,ref}$
	`CoVolume <float>`	Co-volume b_g
	`AttractivePressureConst <float>`	Pressure constant B_g
	`MolecularWeight <float>`	Molecular weight $\mathcal{M}_\mathrm{g}$ of a gas molecule
	`MolecularDiameter <float>`	Kinematic diameter $\mathcal{D}_\mathrm{g}$ of a gas molecule
	`SpecificHeatCapacity <float>`	*Isochoric* specific heat capacity c_v
	`ThermalConductivity <string> <float> <float>`	Kinematic diameter $\mathcal{D}_\mathrm{g}$ of a gas molecule

The influence of the surface tension, the rheology of the lipid-monolayer coating and the viscous dissipation in the liquid is accounted for through the definition of the liquid pressure at the bubble wall, given as [9]

$$p_\mathrm{L} = p_\mathrm{G} - \frac{2\sigma}{R} - 4\,\mu_\ell \frac{\dot{R}}{R} - 4\,\kappa_\mathrm{s} \frac{\dot{R}}{R^2}, \tag{3.21}$$

where σ is the surface tension coefficient, μ_ℓ is the dynamic viscosity of the liquid and κ_s is the surface dilatational viscosity of the lipid monolayer. The clean gas-liquid interface has a surface tension coefficient of $\sigma = \sigma_\mathrm{c}$ and a surface dilatational viscosity of $\kappa_\mathrm{s} = 0$.

The surface tension coefficient is given by the model introduced by Marmottant *et al.* [9] as

$$\sigma = \begin{cases} 0 & \text{for } R \leq R_\mathrm{buck} \\ \chi\left(\dfrac{R^2}{R_\mathrm{buck}^2} - 1\right) & \text{for } R_\mathrm{buck} < R < R_\mathrm{rupt} \\ \sigma_\mathrm{c} & \text{for } R \geq R_\mathrm{rupt} \end{cases} \tag{3.22}$$

where χ is the surface elasticity of the lipid monolayer. When the radius of the bubble becomes smaller than [11]

$$R_\mathrm{buck} = \frac{R_0}{\sqrt{1 + \sigma_0/\chi}}, \tag{3.23}$$

where σ_0 is the surface tension coefficient of the lipid-coated bubble at $R = R_0$, the lipid monolayer cannot compress any further and begins to buckle, as a result of which the surface tension effectively vanishes. In contrast, when the bubble expands to a radius larger than

$$R_\mathrm{rupt} = R_\mathrm{buck}\sqrt{1 + \frac{\sigma_\mathrm{c}}{\chi}}, \tag{3.24}$$

the lipid monolayer ruptures and, as a consequence, the clean gas-liquid interface is laid bare.

The radius-dependent surface tension coefficient of the Marmottant model [9], defined in Eq. (3.22), contains two discontinuities at $R = R_\mathrm{buck}$ and $R = R_\mathrm{rupt}$, where the surface dilatational modulus, $-R^2\,\partial\sigma/\partial(R^2)$, of the lipid monolayer is singular. These discontinuities render the Marmottant model sensitive to the applied time-step when numerically solving the primary ordinary differential equation [15]. A continuously differentiable form of the Marmottant model is constructed using a Gompertz function of the form $f(x) = a\,\mathrm{e}^{-b\,\mathrm{e}^{-cx}}$, a special case of the generalised logistics function, with the surface tension coefficient defined as

$$\sigma = \sigma_\mathrm{c}\,\mathrm{e}^{-b\,\mathrm{e}^{c(1-R/R_\mathrm{buck})}}, \tag{3.25}$$

with $a = \sigma_\mathrm{c}$ and $x = R/R_\mathrm{buck} - 1$, and where the buckling radius R_buck is given by Eq. (3.23). The derivative of the surface tension coefficient follows as

$$\dot\sigma = \sigma\,b\,c\,\mathrm{e}^{c(1-R/R_\mathrm{buck})}\,\frac{\dot R}{R}. \tag{3.26}$$

Enforcing σ_0 for R_0, the coefficient b is readily given as

$$b = -\frac{\ln(\sigma_0/\sigma_\mathrm{c})}{\mathrm{e}^{c(1-R_0/R_\mathrm{buck})}}. \tag{3.27}$$

Assuming, additionally, that the maximum slope of the Gompertz function is equal to the derivative of the surface tension coefficient given by the Marmottant model at $R = R_\mathrm{buck}\sqrt{1 + \sigma_\mathrm{c}/(2\chi)}$, the coefficient c follows as

$$c = \frac{2\chi\mathrm{e}}{\sigma_\mathrm{c}}\sqrt{1 + \frac{\sigma_\mathrm{c}}{2\chi}}. \tag{3.28}$$

Figure 3.1 shows the Marmottant-Gompertz model alongside the Marmottant model for $\sigma_0 = 0.020\,\mathrm{N/m}$, $\sigma_\mathrm{c} = 0.072\,\mathrm{N/m}$ and $\chi = 0.5\,\mathrm{N/m}$, properties that are representative for the bubbles considered in this study. The Marmottant-Gompertz model reproduces the main features of the original Marmottant model, but with a smooth transition between the surface tension regimes, using the same set of input parameters (σ_0, σ_c, χ) and is, therefore, particularly suited to determine the influence of the discontinuities of the original Marmottant model. Furthermore, it provides a good qualitative approximation of the elastic behaviour of the lipid monolayer observed in experiments [14], with a more rapid change of σ near R_buck than near R_rupt.

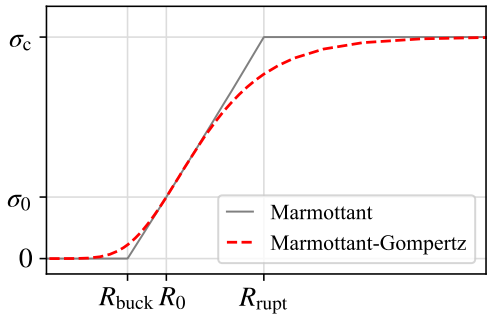

Figure 3.1: Comparison of the radius-dependent surface tension coefficient for lipid monolayers given by the model of Marmottant *et al.* [9], Eq. (3.22), and the Marmottant-Gompertz model, Eq. (3.25), for $\sigma_0 = 0.02\,\mathrm{N/m}$, $\sigma_c = 0.072\,\mathrm{N/m}$ and $\chi = 0.5\,\mathrm{N/m}$. The initial radius R_0, the buckling radius R_{buck}, the rupture radius R_{rupt}, the initial surface tension coefficient σ_0 and the surface tension coefficient of the clean gas-liquid interface, σ_c, are shown as a reference.

3.5 Infinity

generalised Gaussian envelope

$$p_\infty = p_0 - \mathrm{e}^{-G}\,\Delta p_a\,\sin(2\pi f_a t), \tag{3.29}$$

with the exponent G defined as

$$G = \left(\frac{2\,t-\tau}{\Sigma\,\tau}\right)^{2\eta}, \tag{3.30}$$

where Σ represents the standard deviation of the Gaussian and $\tau = t_{end} - t_{start}$ is the width of the envelope, i.e. the duration of the excitation. The power η defines the shape of the envelope, with $\eta = 1$ corresponding to a Gaussian curve and $\eta = \infty$ yielding a rectangular envelope. The derivative of the pressure at infinity is given as

$$\dot{p}_\infty = 2\,\mathrm{e}^{-G}\,\Delta p_a\left[\frac{2\,\eta\,G\,\sin(2\pi f_a t)}{2\,t-\tau} - \pi\,f_a\,\cos(2\pi f_a t)\right] \tag{3.31}$$

For a sinusoidal excitation it is also possible to apply the sum of an arbitrary number N of multiples a of the excitation frequency f_a, with the pressure at infinity defined as

$$p_\infty = p_0 - \Delta p_a \sum_{i=1}^{N} \sin(2\pi a_i f_a t), \tag{3.32}$$

or, including a Gaussian envelope, as

$$p_\infty = p_0 - \mathrm{e}^{-G}\,\Delta p_a \sum_{i=1}^{N} \sin(2\pi a_i f_a t), \tag{3.33}$$

with $0 \leq a_i \leq \infty$ the factor with which the excitation frequency is multiplied. The derivatives follow as

$$\dot{p}_\infty = -2\,\Delta p_a\,\pi\,f_a \sum_{i=1}^{N} a_i\,\cos(2\pi a_i f_a t), \tag{3.34}$$

and

$$\dot{p}_\infty = 2\,\mathrm{e}^{-G}\,\Delta p_a\left[\frac{2\,\eta\,G}{2\,t-\tau}\sum_{i=1}^{N}\sin(2\pi a_i f_a t) - \pi\,f_a\sum_{i=1}^{N} a_i\,\cos(2\pi a_i f_a t)\right], \tag{3.35}$$

respectively.

3.6 Solver

Chapter 4

Acoustic emissions

...

Bibliography

[1] Brenner, M. P., Hilgenfeldt, S., and Lohse, D. (2002). Single-bubble sonoluminescence. *Reviews of Modern Physics*, **74**(2), 425–484.

[2] Denner, F. (2021). The Gilmore-NASG model to predict single-bubble cavitation in compressible liquids. *Ultrasonics Sonochemistry*, **70**, 105307.

[3] Dormand, J. and Prince, P. (1980). A family of embedded Runge-Kutta formulae. *Journal of Computational and Applied Mathematics*, **6**(1), 19–26.

[4] Gilmore, F. R. (1952). The growth or collapse of a spherical bubble in a viscous compressible liquid. Technical Report 26-4, California Institute of Technology, Pasadena, California, USA.

[5] Gümmer, J., Schenke, S., and Denner, F. (2021). Modelling Lipid-Coated Microbubbles in Focused Ultrasound Applications at Subresonance Frequencies. *Ultrasound in Medicine & Biology*, **47**(10), 2958–2979.

[6] Keller, J. B. and Miksis, M. (1980). Bubble oscillations of large amplitude. *The Journal of the Acoustical Society of America*, **68**(2), 628–633.

[7] Lauterborn, W. and Kurz, T. (2010). Physics of bubble oscillations. *Reports on Progress in Physics*, **73**(10), 106501.

[8] Le Métayer, O. and Saurel, R. (2016). The Noble-Abel Stiffened-Gas equation of state. *Physics of Fluids*, **28**(4), 046102.

[9] Marmottant, P., van der Meer, S., Emmer, M., Versluis, M., de Jong, N., Hilgenfeldt, S., and Lohse, D. (2005). A model for large amplitude oscillations of coated bubbles accounting for buckling and rupture. *The Journal of the Acoustical Society of America*, **118**(6), 3499–3505.

[10] Neppiras, E. A. (1980). Acoustic cavitation. *Physics Reports*, **61**(3), 159–251.

[11] Overvelde, M., Garbin, V., Sijl, J., Dollet, B., de Jong, N., Lohse, D., and Versluis, M. (2010). Nonlinear Shell Behavior of Phospholipid-Coated Microbubbles. *Ultrasound in Medicine & Biology*, **36**(12), 2080–2092.

[12] Prosperetti, A. and Lezzi, A. (1986). Bubble dynamics in a compressible liquid. Part 1. First-order theory. *Journal of Fluid Mechanics*, **168**, 457–478.

[13] Radulescu, M. I. (2020). Compressible flow in a Noble–Abel stiffened gas fluid. *Physics of Fluids*, **32**(5), 056101.

[14] Segers, T., Gaud, E., Versluis, M., and Frinking, P. (2018). High-precision acoustic measurements of the nonlinear dilatational elasticity of phospholipid coated monodisperse microbubbles. *Soft Matter*, **14**(47), 9550–9561.

[15] Versluis, M., Stride, E., Lajoinie, G., Dollet, B., and Segers, T. (2020). Ultrasound Contrast Agent Modeling: A Review. *Ultrasound in Medicine & Biology*, **46**(9), 2117–2144.